ACS OMEGA

Open Access

http://pubs.acs.org/journal/acsodf

Article

Semisynthesis of Novel Dispiro-pyrrolizidino/thiopyrrolizidino-oxindolo/indanedione Natural Product Hybrids of Parthenin Followed by Their Cytotoxicity Evaluation

Chetan Paul Singh, Priyanka Sharma, Manzoor Ahmed, Diljeet Kumar, Yogesh Brijwashi Sharma, Jayanta Samanta, Zabeer Ahmed, Sanket Kumar Shukla, Abhijit Hazra,* and Yogesh P. Bharitkar*

Cite This: *ACS Omega* 2023, 8, 35283−35294

Read Online

ACCESS | Metrics & More | Article Recommendations | Supporting Information

ABSTRACT: Natural products possess unique and broader intricacies in the chemical space and have been essential for drug discovery. The crucial factor for drug discovery success is not the size of the library but rather its structural diversity. Although reports on the number of new structurally diverse natural products (NPs) have declined recently, researchers follow the next logical step: synthesizing natural product hybrids and their analogues using the most potent tool, diversity-oriented synthesis (DOS). Here, we use weed *Parthenium hysterophorus* as a source of parthenin for synthesis of novel dispiro-pyrrolizidino/thiopyrrolizidino-oxindolo/indanedione natural product hybrids of parthenin via chemo-, regio-, and stereoselective azomethine ylide cycloaddition. All synthesized compounds were characterized through a detailed analysis of one-dimensional (1D) and two-dimensional (2D) NMR and HRMS data, and the stereochemistries of the compounds were confirmed by X-ray diffraction analysis. All compounds were evaluated for their cytotoxicity against four cell lines (HCT-116, A549, Mia-Paca-2, and MCF-7), and compound **6** inhibited the HCT-116 cells with an IC_{50} of 5.0 ± 0.08 μM.

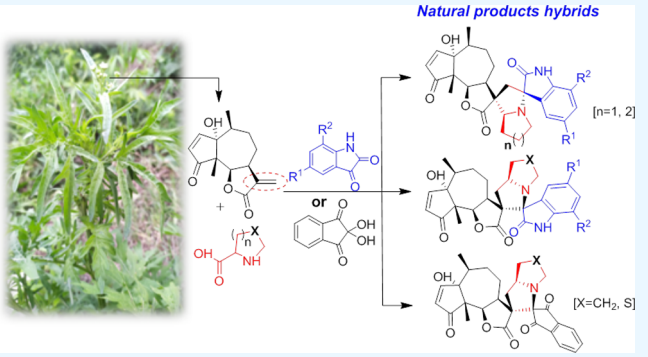

INTRODUCTION

Natural products are traditionally essential sources of medicines in modern drug discovery.[1] Nature synthesizes highly diverse chemicals in plants and microbes for their defense mechanisms.[2] Although a diverse structural motif from nature is the main inspiration for drug discovery, identification and the diversity of new chemical entities (NCEs) from nature in recent years is declining in number.[3] Structurally diverse natural products are the primary source of leads in drug discovery using many approaches like the modern combinatorial chemistry approach,[4,5] natural product hybridization,[6] and evaluation of new chemical libraries using high-throughput screening[7] (HTS) techniques. The next logical step would be to use nature's structural diversity by combining natural products with diverse bioactive moieties to form semisynthetic hybrids with a partial structure of natural products or analogues. Many natural products and semisynthetic natural product analogues/derivatives have been effectively formulated for clinical application to treat human diseases in several therapeutic areas.[8,9] Diversity-oriented synthesis (DOS) has provided commanding probes to explore biological mechanisms and assisted in setting a new goal for advancing synthetic organic chemistry.[10,11] As such, it is essential to understand that the crucial factor for drug discovery success is not the size of the library but its structural diversity.[10]

In this connection, the [1,3] dipolar cycloaddition of alkene or alkyne is an efficient and powerful synthetic tool for the construction of diversified spiro-oxindolo-pyrrolidine rings containing heterocyclic systems, organic catalysts, building blocks, alkaloids, and semisynthetic natural product hybrids in organic chemistry.[11−15] Spirooxindoles find many biological applications as antimicrobials, antileishmanials, antitumorals, inhibitors of NK-1, and so forth and establish the main framework of many biologically active compounds, mainly alkaloids like spirotryprostatine A and B, horsifiline, elacomine, etc.[16−19] In addition, spiroxindoles act as anticancer agents through potential inhibitors of p53-MDM2. Currently, APG-115, DS-3032b, and SAR405838 are in clinical trials as potent inhibitors of p53-MDM2, so spiroxindole is attracting much attention as a p53-MDM2 inhibitor.[20−25]

We have applied our established 1,3 dipolar cycloaddition methodology to several well-known natural products like

Received: July 14, 2023
Accepted: September 5, 2023
Published: September 14, 2023

Scheme 1. Synthesis of Novel Dispiro-oxindole/indanedione Hybrids of Parthenin Using L-Proline

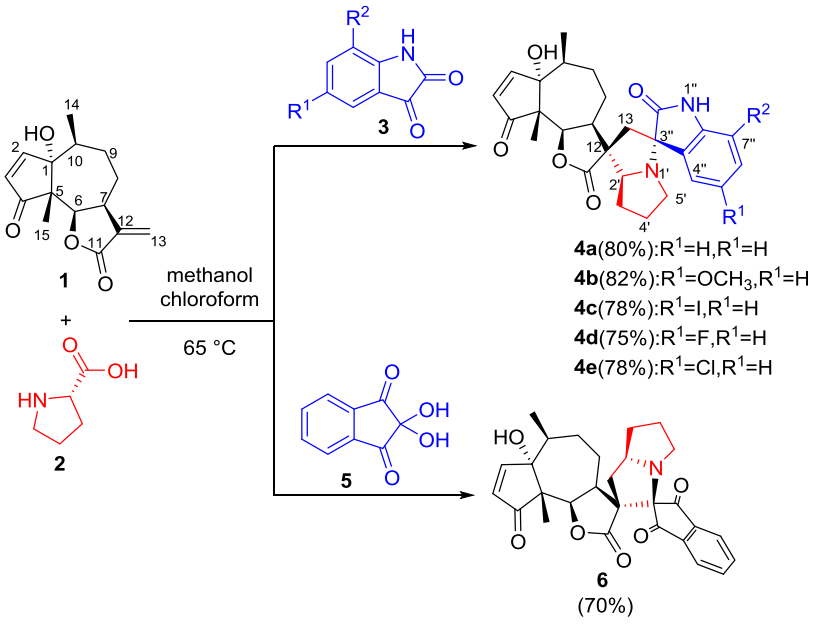

andrographolide, withaferin A, curcumin, piperine, and ixoside, and a collection of novel dispiro/spiro-fused oxindole analogues has been organized. Biological activity evaluation shows a promising increment in activity, and several works are ongoing to derive many newer analogues using these natural products.[26−32]

Parthenin hysterophorous is medicinally utilized as an anticancer, anti-inflammatory, microbicidal, antileishmanial, antitrypanosomal, antiamoebic, and herbicidal agent; a muscle relaxant; a menstrual stimulator; etc.[33,34] Despite being recognized as a weed, *P. hysterophorus* has recently been studied for its application in nanomedicine; as a biopesticide, an agent for bioremediation of poisonous metals and dyes, a herbicide, a cheap substrate for enzyme production; for its potential to produce green manure; and as a source of biogas.[35] To address the existing knowledge gap on *Parthenium hysterophorus*, research must be encouraged to explore its bioactive potential and effectiveness. Herein, we intend to remediate the medicinal value of this weed (*P. hysterophorus*) by using it as a rich source of chemicals such as parthenin, a sesquiterpene lactone. Parthenin shows medicinal properties such as antileishmanial, anticancer, microbicidal, anti-inflammatory, antiviral, and trypanocidal activities.[36−38]

Interestingly, parthenin, the major compound available in *P. hysterophorus*, also contains two diene motifs that might be targeted in a semisynthetic way to generate a library of bioactive dispiropyrrolidinyl oxindoles via 1,3 dipolar cycloaddition. The approach involves utilizing the PAINS motif of parthenin, which includes an α, β unsaturated double bond/Michael acceptor, to add new bioactive motifs. This process aims to reduce toxicity, increase specificity, and improve the physicochemical properties. The diversified library of parthenin hybrids could be utilized efficiently for lead identification in drug discovery. This article describes the chemo-, regio-, and stereoselective synthesis of novel dispiro-pyrrolizidino-oxindolo/dispiro-indenedione natural product hybrids of parthenin via azomethine ylide cycloaddition and their cytotoxicity evaluation.

RESULTS AND DISCUSSION

Synthesis and Characterization of Natural Product Hybrids of Parthenin. Chemically pure parthenin was isolated from the chloroform extract of the *P. hysterophorus* flower and utilized for azomethine ylide dipolar cycloaddition. The one-pot reaction proceeds under milder reaction conditions. Three reactants, parthenin (the electron-deficient double bond substrate), and equimolar quantity of isatin derivatives/ninhydrin (the diketo part) and L-proline/L-thioproline/L-pipecolic acid/sarcosine (the amino acid part) were mixed in a 1:1 ratio of methanol:chloroform (6:4) mixture under reflux for about 8 h to form the products in moderate to good yields. At the outset, L-proline was used as the secondary amino acid to obtain five novel dispiro-oxindole adducts and one dispiro-indanedione adduct of parthenin with an isolated yield of 75−82% (Scheme 1). Further, we tried a reaction in a 1:2:2 mol ratio (parthenin:proline:isatin) via the *in situ* generation of azomethine ylides and observed that one mole was utilized for product formation.

Detailed HRMS and 1D and 2D NMR spectroscopic analyses characterized cycloaddition product **4a**. Compound **4a** showed the desired quasi-molecular ion peaks at 463.2235 $[M + H]^+$. While the ^{13}C NMR spectra of parthenin (**1**) showed 15 carbon signals, the ^{13}C NMR spectra of **4a** showed 27 carbon signals, with nine C, ten CH, six CH_2, and two CH_3, clearly indicating the formation of the desired dispiro-oxindole hybrids of parthenin.

A further thorough observation of ^{13}C NMR signals of the C-12 and C-13 exocyclic double bond indicated the upfield shifting from δ 141.3 (C-12) and δ 120.88 (C-13) to δ 62.4 (C-12; spiro carbon of the lactone ring) and δ 36.59 (C-13) after cycloaddition. The HMBC cross peaks between oxindole carbonyl carbon δ 180.9 (C-2″) and both protons δ 3.24 (dd, J = 12.8, 9.4 Hz) and 2.37 (m) of the $-CH_2$ (δ 36.59, C-13) carbon confirmed α-addition of ylide on the exocyclic double bond. The absolute configuration of **4a** was established by single-crystal X-ray diffraction analysis, and the structure is shown in Figure 1.

https://doi.org/10.1021/acsomega.3c05020
ACS Omega 2023, 8, 35283−35294

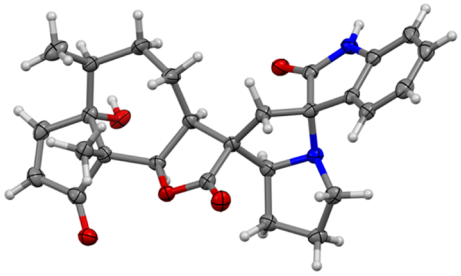

Figure 1. Molecular structure of **4a** as determined by SCXRD analysis. Thermal ellipsoids are shown at the 50% probability level (CCDC No. 2279212).

Similarly, adduct **6** was synthesized successfully using ninhydrin and proline with parthenin (Scheme 1) and characterized by detailed mass, NMR, and 2D NMR (HMBC and COSY) analyses. The HMBC cross peaks between the δ 4.17 proton (dd, J = 11.5, 6.6 Hz, of 46.19, C-7) and both the spiro carbon of the indanedione ring, δ 81.52 (C-2″), and that of the lactone ring, δ 66.83 (C-12), confirmed the β addition of azomethine ylide with the exocyclic double bond, and the molecular structure was further confirmed by X-ray diffraction, as shown in Figure 2. Interestingly, in this case, an alteration in regiochemistry was observed due to the β-addition of the ylide on the exocyclic double bond.

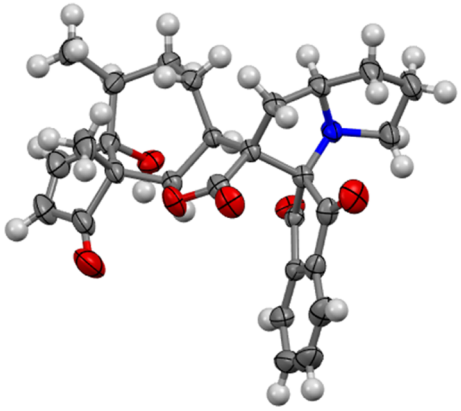

Figure 2. Molecular structure of **6** as determined by SCXRD analysis. Thermal ellipsoids are shown at the 50% probability level (CCDC No. 2269152).

Similarly, using thioproline (L-thiazolidine 4-carboxylic acid) and isatin derivatives, novel thiopyrrolizidino dispiro-oxinolo parthenin hybrid analogues (**8a−e**) were synthesized (Scheme 2). Thiopyrrolizidino dispiro-indanedione parthenin hybrid (**9**) was also synthesized successfully. Product **8e** was characterized by a detailed analysis of mass spectrometry and HRMS and 1D and 2D NMR data. Compound **8e** showed an expected pseudomolecular ion peak at 559.0904 $[M + H]^+$. The ^{1}H and ^{13}C NMR spectra showed the expected number of protons and carbons. The ^{13}C NMR and DEPT analyses found 26 carbon signals in ^{13}C NMR, with ten C, nine CH, five CH_2, and two CH_3. The cycloaddition that occurred at the exocyclic double bond has been confirmed by the upfield shifting of ^{13}C NMR signals of the exocyclic double bond from δ 141.3 (C-12) and δ 120.88 (C-13) to δ 65.14 (C-12) and 35.4 (C-13), respectively, after product formation. Similar HMBC cross peaks between the δ 3.98 proton (dd, J = 11.4, 5.5 Hz, 1H; 48.26, C-7) and both the spiro carbon of the oxindole ring, δ 75.19 (C-3″), and that of the lactone ring, δ 65.14 (C-12), confirmed the β cycloaddition similar to **6**. Single-crystal X-ray diffraction analysis of compounds **8d** and **8e** confirmed the absolute configurations and stereochemical arrangements, as shown in Figure 3. Similarly, adduct **9** was synthesized successfully using ninhydrin, thioproline, with parthenin (Scheme 2) and characterized by a detailed mass NMR analysis. Similar regiochemistry to **8d** and **8e** was confirmed by HMBC analysis, and further confirmation was done by single-crystal X-ray diffraction analysis of compound **9** (Figure 4).

To introduce additional diversity in dispiro-oxindole adducts of parthenin (with substituents or different ring systems), we used another secondary amino acid, L-pipecolic acid (piperidine-2-carboxylic acid), to generate azomethine ylide followed by the synthesis of diverse novel cycloadduct **10a−e** (Scheme 3), and all of the synthesized compounds were characterized by extensive analysis of HRMS and ^{1}H and ^{13}C NMR data. Cycloaddition product **10a**, obtained from the reaction, was characterized by a detailed analysis of HRMS and 1D and 2D NMR data. Compound **10a** showed desired quasi-molecular ion peaks at 477.2389 $[M + H]^+$. While 15 carbon signals were observed in the ^{13}C NMR spectra of parthenin (**1**), **10a** shows 28 carbon signals, with nine C, ten CH, seven CH_2, and two CH_3. Just like the previous products, upfield shifting of the ^{13}C NMR signals of the exocyclic double bond was observed from δ 141.3 (C-12) and δ 120.88 (C-13) to δ 60.99 (C-12) and 34.52 (C-13), respectively, in **10a**. This indicates the formation of the cycloadduct shown in Scheme 3. The HMBC cross peaks between oxindole carbonyl carbon δ 179.0 (C-2″) and both protons δ 2.89 (dd, J = 12.4, 9.2 Hz) and 2.24 of the $-CH_2$ carbon (δ 33.91) confirmed α-addition of ylide on the exocyclic double bond. During a reaction with parthenin, pipecolic acid, and ninhydrin, we did not observe compound **11**.

The successful synthesis of a novel diverse natural product hybrid of parthenin, with three cyclic secondary amino acids, has encouraged us to try sarcosine, the acyclic secondary amino acid. The desired products **13a−e** and **14** were synthesized (Scheme 4). From the reaction with 5-methyl isatin, product **13c** was characterized by detailed analysis of mass spectrometry, HRMS, and 1D and 2D NMR data. Compound **13c** showed an expected pseudomolecular ion peak at 451.2232 $[M + H]^+$ for molecular formula $C_{26}H_{30}N_2O_5$. The ^{1}H and ^{13}C NMR spectra showed the expected number of protons and carbons. The ^{13}C NMR and DEPT analyses found 26 carbon signals in ^{13}C NMR, with ten C, eight CH, four CH_2, and four CH_3. The signals of the exocyclic double bond of parthenin (**1**) shifted from δ 141.3 (C-12) and 120.88 (C-13) to δ 61.62 (C-12) and 28.03 (C-13), respectively. The HMBC showed the correlation between δ [3.54−3.51 (m); 48.3, C-7] and both spiro carbon of oxindole ring δ 75.19 (C-3″) and spiro carbon of lactone ring δ 62.62 (C-12), concludes the β addition of azomethine ylide with the exocyclic double bond of the parthenin. A further conclusion was made based on the similar regiochemistry of products with a comparison of **6**, **8a−e**, and **9**. Then, a final conclusion about the absolute configuration of the compound was confirmed by X-ray analysis of compound **14**, as shown in Figure 5.

All of the cycloaddition reactions proceeded chemoselectively and diastereoselectively, as the exocyclic double

https://doi.org/10.1021/acsomega.3c05020
ACS Omega 2023, 8, 35283−35294

Scheme 2. Synthesis of Novel Dispiro-oxindolo/indanedione Hybrids of Parthenin Using L-Thiazolidine-4-carboxylic Acid (Thioproline)

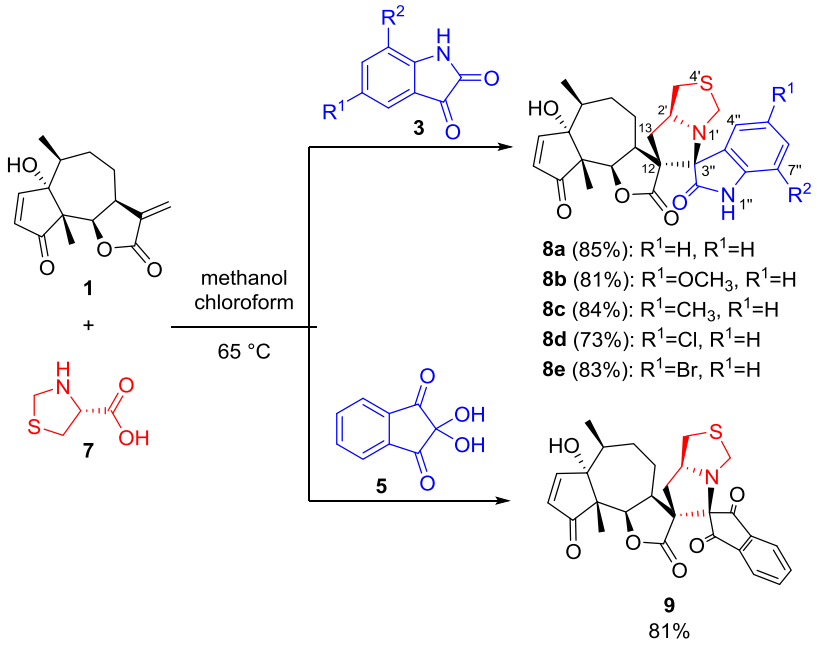

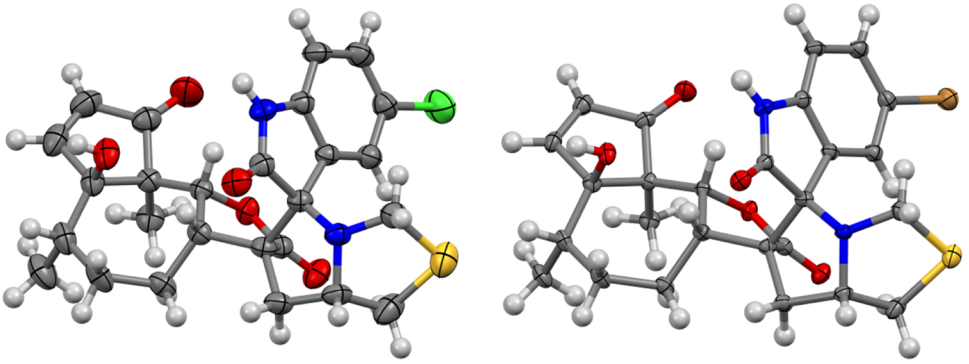

Figure 3. Molecular structures of **8d** and **8e** as determined by SCXRD analysis. Thermal ellipsoids are shown at the 50% probability level (CCDC No. 2269153 and CCDC No. 2269151).

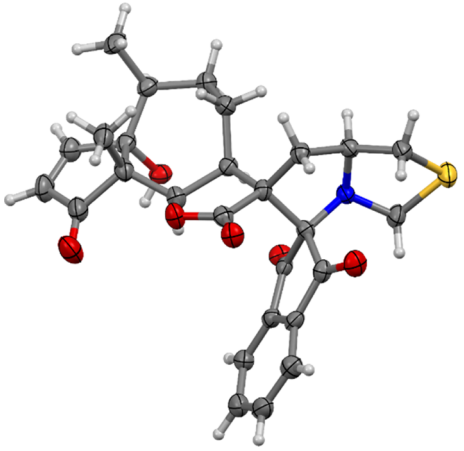

Figure 4. Molecular structure of **9** as determined by SCXRD analysis. Thermal ellipsoids are shown at the 50% probability level (CCDC No. 2269149).

bond of parthenin participated in the reaction but not the endocyclic double bond. A change in the regiochemistry of products was observed due to a change in the amino acid from L-proline and L-pipecolic acid to L-thioproline and sarcosine, as confirmed by X-ray analysis and detailed NMR study.

Cytotoxicity Evaluation. Parent molecule parthenin and all synthesized hybrids were initially screened for cytotoxicity potential using the sulforhodamine-B (SRB) assay. Four different cancer cell lines were used, including HCT-116 (colon), A549 (lungs), Mia-Paca-2 (pancreas), and MCF-7 (breast) at two concentrations of 10 and 50 μM. Camptothecin was used as a positive control in this assay. The detailed cytotoxic effect of each compound against different cancer cell lines at 10 and 50 μM is given in Table S1. Further, compounds with more than 50% inhibition at 10 μM were evaluated for their half-maximal inhibitory concentration (IC_{50} value). Among the entire cell lines, compound **6** inhibited the HCT-116 cells with an IC_{50} of 5.0 ± 0.08 μM, as displayed in Table 1.

CONCLUSIONS

In summary, we synthesized 23 novel dispiro-pyrrolizidino/thiopyrrolizidino-oxindolo/indanedione natural product hy-

https://doi.org/10.1021/acsomega.3c05020
ACS Omega 2023, 8, 35283−35294

Scheme 3. Synthesis of Novel Dispiro-oxindolo/indanedione Hybrids of Parthenin Using L-Pipecolic Acid

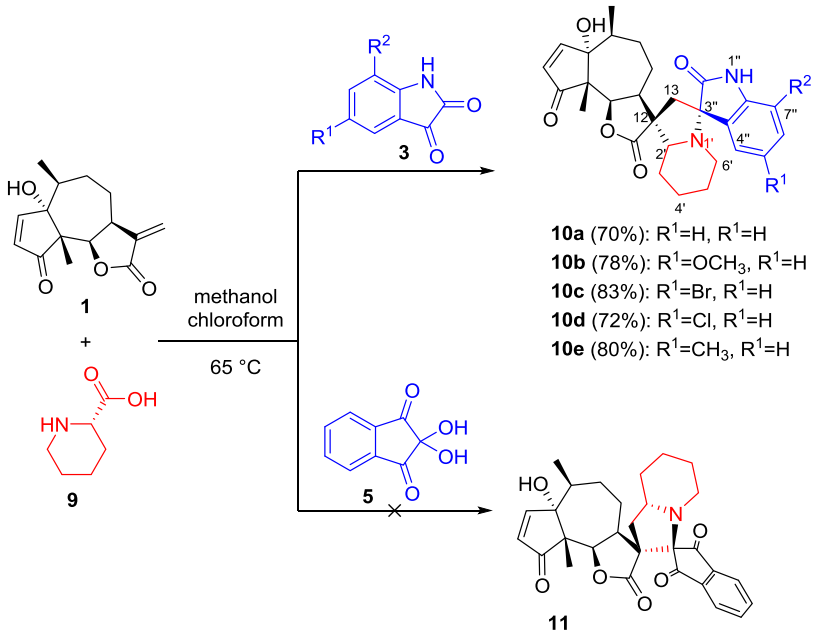

Scheme 4. Synthesis of Novel Dispiro-oxindolo/indanedione Hybrids of Parthenin Using Sarcosine

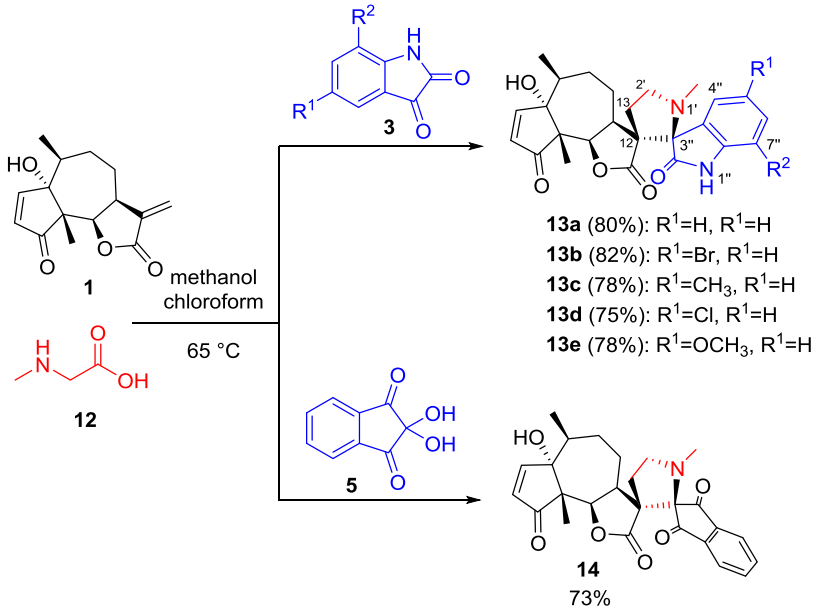

brids of parthenin via 1,3 dipolar azomethine ylide cycloaddition. The cycloaddition reactions proceeded in a chemo- and diastereoselective way, as only C-12 and C-13 exocyclic double bonds reacted, while C-2 and C-3 endocyclic double bonds remained unreacted. The synthesized compounds also showed regioselective cycloaddition; with azomethine ylide, α-addition was observed in the case of L-proline and L-pipecolic acid, while β-addition was observed in the case of thioproline and sarcosine. It was also observed that cycloaddition between the exocyclic double bond of parthenin and ylide of proline-ninhydrine showed β-addition. All synthesized compounds were extensively characterized by HRMS and 1D and 2D NMR, and the stereochemistry of compounds was confirmed by X-ray analysis. All compounds were evaluated for their cytotoxicity against four cell lines (HCT-116, A549, Mia-Paca-2, and MCF-7), and compound **6** inhibited the HCT-116 cells with an IC_{50} of 5.0 ± 0.08 μM. The synthesis of diversified spiropyrrolidinyl-oxindole/indanedione systems from the natural product parthenin as the substrate could be of utmost importance to drug discovery, medicinal and natural product chemistry, and health sciences.

EXPERMENTAL SECTION

General. Parthenin was isolated from the chloroform extract of the flower of *P. hysterophorous* by column chromatography and crystallization. All reaction chemicals and solvents were purchased from commercial sources and used as received without further purification unless otherwise indicated. Thin-layer chromatography (TLC) analysis was performed on Merck 60 F_{254} silica gel TLC plates using a

https://doi.org/10.1021/acsomega.3c05020
ACS Omega 2023, 8, 35283−35294

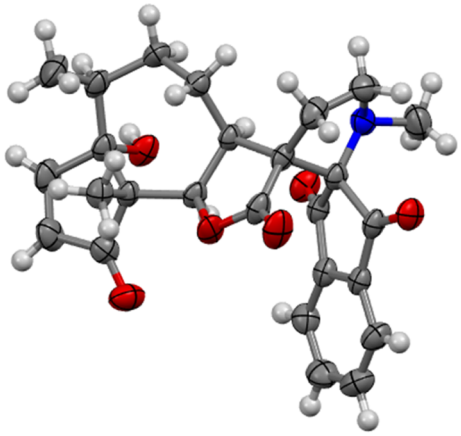

Figure 5. Molecular structure of **14** as determined by SCXRD analysis. Thermal ellipsoids are shown at the 50% probability level (CCDC No. 2269150).

solvent system of 1−2% methanol in chloroform, and spots were identified using an ultraviolet (UV) indicator (254 nm) followed by staining by iodine vapors. The NMR spectra were recorded by a Bruker 400 DPX using deuterated solvents like pyridine-d_5. HRMS spectra of compounds were obtained using an Agilent 6545 Q-TOF liquid chromatography/mass spectrometry (LC/MS) instrument. Roswell Park Memorial Institute (RPMI)-1640 medium, Dulbecco's modified Eagle's medium (DMEM), phosphate-buffered saline (PBS), and sulforhodamine-B (SRB) were purchased from Sigma-Aldrich Co. (St. Louis, MO). Fetal bovine serum (FBS) was obtained from Thermo Scientific (Rockford).

Isolation and Purification of Parthenin. *P. hysterophorous* flowers were collected from the CSIR-IIIM Jammu campus and shade-dried. Three kilograms of shade-dried flowers was percolated in chloroform and extracted successively thrice with chloroform. Column chromatography of the crude chloroform extract was performed over silica gel (100−200 mesh). The column was packed by using silica gel in hexane and eluted successively with hexane, hexane−chloroform, and chloroform. All of the fractions were collected, separately evaporated to dryness, and spotted on TLC using the benzene:chloroform:ethyl acetate (6:3:1) solvent system. Fractions showing homogeneous spots matching with the standard were mixed, concentrated, and crystallized in methanol.

Synthesis. Parthenin (1.90 mmol/, 500 mg), isatin (2.28 mmol, 336.5 mg), and proline (2.28 mmol, 263 mg) were combined and dissolved in 50 mL of a 60:40 mixture of methanol and chloroform and then heated to reflux for about 8 h. The completion of the reaction was concluded by TLC, the solvent was removed by a rotavapor, and the crude reaction mixture was subjected to column chromatography using silica gel (100−200mesh) eluted with 2% methanol in chloroform and crystallized in methanol. All other compounds (**1**, **4a**−**4e**, **6**, **8a**−**8e**, **9**, **10a**−**10e**, **13a**−**13e**, and **14**) were synthesized using similar processes and characterized by ^{1}H and ^{13}C NMR, 2D NMR, and HRMS spectral data described in the Supporting File.

Spectral Data. *Compound* ***1***. Colorless needle-shaped crystals: HRMS [ESI-MS, positive mode]: MF: $C_{15}H_{18}O_4$; observed m/z 285.1098 [M + H] $^+$ [calcd. 285.1103]; ^{1}H NMR (400 MHz, pyridine-d_5): δ 7.69 (d, J = 5.9 Hz, 1H), 7.33 (s, 1H), 6.39 (d, J = 2.4 Hz, 1H), 6.27 (d, J = 5.8 Hz, 1H), 5.60 (d, J = 2.4 Hz, 1H), 5.43 (d, J = 7.9 Hz, 1H), 3.71−3.58 (m, 1H), 2.50−2.36 (m, 2H), 1.84−1.77 (m, 1H), 1.64−1.56 (m, 1H), 1.34 (s, 3H), 1.04 (d, J = 7.6 Hz, 3H); ^{13}C NMR (100 MHz, Pyridine-d_5): δ 211.10 (−C═O), 170.73 (−C═O), 164.37(−CH), 144.63 (−C), 130.88 (−CH), 120.87-(−CH_2), 83.65 (−C), 79.37 (−CH), 59.52 (−C), 44.54 (−CH), 40.93 (−CH), 30.15(−CH_2), 28.66 (−CH_2), 18.30 (−CH_3), 17.20 (−CH_3).

Compound ***4a***. Colorless needle-shaped crystals; melting point: 237−238 °C; isolated yield: 881 mg (80%); HRMS [ESI-MS, positive mode]: MF: $C_{27}H_{30}N_2O_5$; observed m/z 463.2235 [M + H] $^+$ [calcd. 463.2233]; ^{1}H NMR (400 MHz, pyridine-d_5): δ 11.81 (1H, s, −NH), 7.95 (d, J = 7.4 Hz, 1H), 7.50 (d, J = 5.9 Hz, 1H), 7.19−7.13 (m, 2H), 7.07 (td, J = 7.6, 1.1 Hz, 1H), 6.62 (d, J = 7.1 Hz, 1H), 6.07 (d, J = 5.9 Hz, 1H), 4.68−4.57 (m, 2H), 3.94−3.82 (m, 1H), 3.55 (ddd, J = 11.7, 6.2, 1.9 Hz, 1H), 3.24 (dd, J = 12.8, 9.4 Hz, 1H), 2.64 (t, J = 6.9 Hz, 1H), 2.59−2.48 (m, 1H), 2.48−2.29 (m, 3H), 2.19−2.09 (m, 1H), 2.07−1.85 (m, 2H), 1.74 (dt, J = 12.4, 6.0 Hz, 1H), 1.62 (dd, J = 13.5, 5.0 Hz, 1H), 1.36 (s, 3H), 1.34−1.21 (m, 2H), 0.98 (d, J = 7.7 Hz, 3H); ^{13}C NMR (100 MHz, pyridine-d_5): δ 211.3 (−C═O), 180.9 (−C═O), 178.5 (−C═O), 164.45(−CH), 144.1 (−C), 130.6 (−CH), 130.0 (−CH), 127.7 (−CH), 125.4 (−CH), 121.8 (−CH), 109.8 (−CH), 83.8 (−C), 79.0 (−CH), 76.99 (−C), 63.46 (−CH), 62.78 (−C), 59.16 (−C), 50.0 (−CH_2), 49.28 (−CH), 40.29 (−CH), 36.59 (−CH_2), 32.6 (−CH_2), 32.0 (−CH_2), 27.7 (−CH_2), 23.48 (−CH_2), 20.5 (−CH_3),17.68(−CH_3).

Compound ***4b***. White powder; melting point: 203−204 °C; isolated yield: 769 mg (82%); HRMS [ESI-MS, positive mode]: MF: $C_{28}H_{32}N_2O_6$; observed m/z 493.2341 [M + H] $^+$ [calcd. 493.2339]; ^{1}H NMR (400 MHz, pyridine-d_5): δ 11.63 (1H, s, −NH), 7.73 (d, J = 2.5 Hz, 1H), 7.50 (d, J = 5.9 Hz, 1H), 7.13 (s, 1H), 6.87 (dd, J = 8.4, 2.5 Hz, 1H), 6.59 (d, J = 8.4 Hz, 1H), 6.59 (d, J = 8.4 Hz, 1H), 4.67−4.60 (m, 2H), 3.93−3.88 (m, 1H), 3.86 (s, 3H), 3.60−3.52 (m, 1H), 3.24 (dd, J = 12.8, 9.3 Hz, 1H), 2.71 (t, J = 6.8 Hz, 1H), 2.60−2.50 (m, 1H), 2.48−2.28 (m, 3H), 2.17−2.09 (m, 1H), 2.06−1.88 (m, 3H), 1.82−1.70 (m, 1H), 1.63 (dd, J = 13.3, 4.7 Hz, 1H), 1.35 (s, 3H), 0.98 (d, J = 7.6 Hz, 3H); ^{13}C NMR (100 MHz, pyridine-d_5): δ 211.93 (−C═O), 181.58 (−C═O), 179.18

Table 1. IC_{50} of Selected Compounds against Selected Cell Lines

code	HCT-116 (μM)	A549 (μM)	Mia-Paca-2 (μM)	MCF-7 (μM)
1	6 ± 0.07	≥30 μM	10.61 ± 0.03	8.6 ± 0.03
6	5.0 ± 0.08	≥30 μM	12.81 ± 0.01	8.67 ± 0.03
8d	12.12 ± 0.12	≥30 μM	22.6 ± 0.06	15.17 ± 0.05
10d	11.1 ± 0.07	23 ± 0.08	17 ± 0.02	13.27 ± 0.06
10c	10.26 ± 0.09	≥30 μM	12.5 ± 0.07	13.74 ± 0.08
camptothecin	0.07 ± 0.04	0.058 ± 0.04	0.08 ± 0.03	0.19 ± 0.08

https://doi.org/10.1021/acsomega.3c05020
ACS Omega 2023, 8, 35283−35294

(−C═O), 165.09 (−CH), 156.23 (−C), 138.12 (−C), 131.29 (−CH), 127.12 (−C), 116.50 (−CH), 115.76 (−CH), 110.73 (−CH), 84.12 (−C), 79.68 (−CH), 77.96 (−C), 64.21 (−CH), 63.58 (−C), 59.79 (−C), 56.83 ($-CH_3$), 50.49 ($-CH_2$), 49.86 (−CH), 40.92 (−CH), 37.09 ($-CH_2$), 33.16 ($-CH_2$), 32.68 ($-CH_2$), 28.37 ($-CH_2$), 24.04 ($-CH_2$), 20.62 ($-CH_3$), 18.34 ($-CH_3$).

Compound ***4c***. White powder; melting point: 220−221 °C; isolated yield: 875 mg (78%); HRMS [ESI-MS, positive mode]: MF: $C_{27}H_{29}IN_2O_5$; observed *m*/*z* 589.1195 $[M + H]^+$ [calcd. 589.1199]; ^{1}H NMR (400 MHz, pyridine-d_5): δ 12.08 (1H, s, −NH), 8.38 (d, *J* = 2.3 Hz, 1H), 7.54−7.46 (m, 1H), 7.30−7.14 (m, 2H), 6.46 (dd, *J* = 19.4, 8.1 Hz, 1H), 6.12−6.01 (m, 1H), 4.66−4.58 (m, 2H), 3.78−3.74 (m, 1H), 3.58−3.56 (m, 1H), 3.21−3.14 (m, 1H), 2.66−2.63 (m, 1H), 2.47−2.34 (m, 4H), 2.15−1.91 (m, 7H), 2.07−1.85 (m, 2H), 1.74 (dt, *J* = 12.4, 6.0 Hz, 1H), 1.62 (dd, *J* = 13.5, 5.0 Hz, 1H), 1.34 (s, 3H), 1.00 (d, *J* = 6.6 Hz, 3H); ^{13}C NMR (100 MHz, pyridine-d_5): δ 211.49 (−C═O), 180.82 (−C═O), 178.25 (−C═O), 164.83(−CH), 144.20 (−C), 139.27 (−CH), 136.38 (−CH), 131.01 (−CH), 128.43 (−C), 112.33 (−CH), 84.94 (−C), 84.13 (−C), 79.51 (−CH), 76.99 (−C), 63.99 (−CH), 63.48(−C), 59.46 (−C), 50.19 ($-CH_2$), 49.37 (−CH), 40.59 (−CH), 36.64 ($-CH_2$), 32.83 ($-CH_2$), 32.41 ($-CH_2$), 28.15 ($-CH_2$), 23.72 ($-CH_2$), 20.27 ($-CH_3$), 18.08($-CH_3$).

Compound ***4d***. White powder; melting point: 255−256 °C; isolated yield: 687 mg (75%); HRMS [ESI-MS, positive mode]: MF: $C_{27}H_{29}FN_2O_5$; observed *m*/*z* 481.2136 $[M + H]^+$ [calcd. 481.2139]; ^{1}H NMR (400 MHz, pyridine-*d*5): δ 11.93 (1H, s, −NH), 7.80 (dd, *J* = 8.8, 2.4 Hz, 1H), 7.53 (d, *J* = 5.9 Hz, 1H), 7.19−7.09 (m, 1H), 7.08−6.93 (m, 1H), 6.58 (dd, *J* = 8.5, 4.5 Hz, 1H), 6.10 (d, *J* = 5.9 Hz, 1H), 4.63−4.59 (m, 2H), 3.77−3.72 (m, 1H), 3.66−3.58 (m, 1H), 3.16 (dd, *J* = 12.9, 9.2 Hz, 1H), 2.64 (t, *J* = 6.8 Hz, 1H), 2.58−2.29 (m, 5H), 2.18−2.07 (m, 2H), 2.05−1.91 (m, 1H), 1.91−1.83 (m, 1H), 1.82−1.71 (m, 1H), 1.63 (dd, *J* = 13.2, 4.6 Hz, 1H), 1.34 (s, 3H), 0.99 (d, *J* = 7.6 Hz, 3H); ^{13}C NMR (100 MHz, pyridine-*d*5): δ 211.3 (−C═O), 180.38 (−C═O), 178.5 (−C═O), 164.57(−CH), 158.47 (−C, $^1J_{C-F}$ = 238.4 Hz), 140.21 (−C), 130.6 (−CH), 127.08 (−C, $^3J_{C-F}$ = 7.5 Hz), 116.4 (−CH, $^2J_{C-F}$ = 23.4 Hz), 115.46 (−CH, $^2J_{C-F}$ = 25.4 Hz), 110.35 (−CH, $^3J_{C-F}$ = 7.9 Hz), 83.78 (−C), 79.06 (−CH), 76.98 (−C), 63.56 (−CH), 63.35 (−C), 59.15 (−C), 49.70 ($-CH_2$), 49.08 (−CH), 40.21 (−CH), 36.32 ($-CH_2$), 32.48 ($-CH_2$), 32.0 ($-CH_2$), 27.73 ($-CH_2$), 23.32 ($-CH_2$), 19.96 ($-CH_3$), 17.67($-CH_3$).

Compound ***4e***. White powder; melting point: 288−289 °C; isolated yield: 738 mg (78%); HRMS [ESI-MS, positive mode]: MF: $C_{27}H_{29}ClN_2O_5$; observed *m*/*z* 497.1842 $[M + H]^+$ [calcd. 497.1843]; ^{1}H NMR (400 MHz, pyridine-*d*5): δ 12.03 (1H, s, −NH), 7.99 (d, *J* = 1.5 Hz, 1H), 7.49 (dd, *J* = 5.9, 1.7 Hz, 1H), 7.24−7.18 (m, 1H), 7.13 (s, 1H), 6.57 (dd, *J* = 8.3, 1.4 Hz, 1H), 6.06 (dd, *J* = 5.9, 1.3 Hz, 1H), 4.60 (d, *J* = 6.1 Hz, 1H), 4.59−4.47 (m, 1H), 3.75−3.64 (m, 1H), 3.55 (dd, *J* = 11.4, 6.1 Hz, 1H), 3.12 (dd, *J* = 12.8, 9.2 Hz, 1H), 2.60 (t, *J* = 6.9 Hz, 1H), 2.48−2.25 (m, 5H), 2.13−2.04 (m, 1H), 2.02−1.78 (m, 3H), 1.72 (qd, *J* = 11.9, 6.1 Hz, 1H), 1.60 (dd, *J* = 12.8, 5.2 Hz, 1H), 1.29 (s, 3H), 0.95 (d, *J* = 7.1 Hz, 3H); ^{13}C NMR (100 MHz, pyridine-d_5): δ 211.9 (−C═O), 181.05 (−C═O), 178.91 (−C═O), 165.23(−CH), 143.57 (−C), 131.32 (−CH), 130.70 (−CH), 128.36 (−CH), 128.08 (−C), 127.48 (−C), 111.67 (−CH), 84.47 (−C), 79.80 (−CH), 77.50 (−C), 64.30 (−CH), 63.94(−C), 59.81 (−C), 50.44 ($-CH_2$), 50.14 (−CH), 49.69 (−CH), 40.90 (−CH), 36.96 ($-CH_2$), 33.14 ($-CH_2$), 32.70 ($-CH_2$), 28.45 ($-CH_2$), 24.02 ($-CH_2$), 20.60 ($-CH_3$), 18.37($-CH_3$).

Compound ***6***. Yellow block crystals; melting point: 201−202 °C; isolated yield: 634 mg (70%); HRMS [ESI-MS, positive mode]: MF: $C_{28}H_{29}NO_6$; observed *m*/*z* 476.2072 $[M + H]^+$ [calcd. 476.2073]; ^{1}H NMR (400 MHz, pyridine-d_5): δ 7.97−7.94 (m, 1H), 7.70−7.68 (m, 2H), 7.60−7.55 (m, 2H), 7.39 (s, 1H), 6.26 (d, *J* = 5.9 Hz, 1H), 4.99 (d, *J* = 6.6 Hz, 1H), 4.17 (dd, *J* = 11.5, 6.6 Hz, 1H), 3.98−3.86 (m, 1H), 2.93−2.76 (m, 3H), 2.57−2.41 (m, 3H), 2.19−2.05 (m, 2H), 1.99−1.87 (m, 3H), 1.78−1.67 (m, 2H), 1.26 (s, 3H), 1.04 (d, *J* = 7.7 Hz, 3H); ^{13}C NMR (100 MHz, pyridine-d_5): δ 212.22 (−C = O), 200.44 (−C═O), 299.63 (−C═O), 176.29 (−C═O), 165.83(−CH), 141.65 (−C), 141.37 (−C), 137.54 (−CH), 137.21 (−CH), 131.41(−CH), 123.84 (−CH), 123.42 (−CH), 84.32 (−C), 81.52 (−C), 80.22 (−CH), 66.83(−C), 65.58(−CH), 60.18(−C), 47.61 ($-CH_2$), 46.19 (−CH), 41.00 (−CH), 35.85 ($-CH_2$), 32.88 ($-CH_2$), 32.53 ($-CH_2$), 30.95 ($-CH_2$), 22.71 ($-CH_2$), 19.97 ($-CH_3$), 18.29 ($-CH_3$).

Compound ***8a***. White powder; melting point: 238−239 °C; isolated yield: 778 mg (85%) HRMS [ESI-MS, positive mode]: MF: $C_{26}H_{28}N_2O_5S$; MF: $C_{26}H_{28}N_2O_5S$; observed *m*/*z* 481.1798 $[M + H]^+$ [calcd. 481.1797]; ^{1}H NMR (400 MHz, pyridine-d_5): δ 12.07 (1H, s, −NH), 7.84 (d, *J* = 7.5 Hz, 1H), 7.55 (dd, *J* = 8.8, 4.0 Hz, 1H), 7.27 (s, 1H), 7.21−7.17 (m, 1H), 7.03−6.99 (m, 1H), 6.09 (t, *J* = 4.9 Hz, 1H), 4.68 (d, *J* = 5.8 Hz, 1H), 4.61−4.52 (m, 1H), 4.04−3.99 (m, 1H), 3.88−3.80 (m, 1H), 3.78−3.73 (m, 1H), 3.60−3.52 (m, 1H), 3.60−3.52 (m, 1H), 3.14−3.08 (m, 1H), 3.00−2.95 (m, 1H), 2.45−2.42 (m, 3H), 2.06−1.92 (m, 1H), 1.67−1.64 (m, 1H), 1.32 (s, 3H), 1.28 (s, 1H), 0.99 (d, *J* = 6.3 Hz, 2H); ^{13}C NMR (100 MHz, pyridine-d_5): δ 211.90 (−C═O), 179.17(−C═O), 178.77 (−C═O), 165.25(−CH), 144.37 (−C), 131.28 (−CH), 131.04 (−CH), 127.73 (−CH), 125.12 (−CH), 122.93(−CH), 110.78 (−CH), 84.48 (−C), 79.44 (−CH), 75.61 (−C), 66.68 (−CH), 65.37 (−C), 59.80 (−C), 49.66 ($-CH_2$), 49.60 (−CH), 40.90 (−CH), 35.85($-CH_2$), 32.70 ($-CH_2$), 30.44 ($-CH_2$), 23.41 ($-CH_2$), 20.72 ($-CH_3$), 18.41($-CH_3$).

Compound ***8b***. White powder; melting point: 259−260 °C; isolated yield: 749 mg (81%); HRMS [ESI-MS, positive mode]: MF: $C_{27}H_{30}N_2O_6S$; observed *m*/*z* 511.1906 $[M + H]^+$ [calcd. 511.1903]; ^{1}H NMR (400 MHz, pyridine-d_5): δ 11.89 (1H, s, −NH), 7.60 (d, *J* = 2.8 Hz, 1H), 7.53 (d, *J* = 5.9 Hz, 1H), 7.27 (s, 1H), 6.91 (dd, *J* = 8.4, 2.6 Hz, 1H), 6.66 (d, *J* = 8.4 Hz, 1H), 6.08 (d, *J* = 5.9 Hz, 1H), 4.74 (d, *J* = 5.8 Hz, 1H), 4.60−4.50 (m, 1H), 4.02 (d, *J* = 6.5 Hz, 1H), 3.89 (dd, *J* = 11.3, 5.5 Hz, 1H), 3.83 (d, *J* = 6.5 Hz, 1H), 3.67 (s, 3H), 3.55 (t, *J* = 9.1 Hz, 1H), 3.11 (dd, *J* = 9.0, 6.0 Hz, 1H), 2.47−2.39 (m, 3H), 2.02−1.91 (m, 1H), 1.83 (dd, *J* = 14.2, 4.7 Hz, 1H), 1.65 (dd, *J* = 13.2, 4.6 Hz, 1H), 1.31 (s, 3H), 0.99 (d, *J* = 7.6 Hz, 3H); ^{13}C NMR (100 MHz, pyridine-d_5): δ 211.84 (−C═O), 179.07(−C═O), 178.78 (−C═O), 165.20(−CH), 156.47(−C), 136.28 (−CH), 131.27 (−CH), 126.27 (−C), 116.82 (−CH), 114.35 (−CH), 111.18 (−CH), 84.47 (−C), 79.46 (−CH), 76.01 (−C), 66.87 (−CH), 65.70 (−C), 59.80 (−C), 56.30 ($-CH_3$), 49.68 (−CH), 49.60 ($-CH_2$), 40.90 (−CH), 35.79 ($-CH_2$), 32.71 ($-CH_2$), 32.62 ($-CH_2$), 23.29 ($-CH_2$), 20.68 ($-CH_3$), 18.41($-CH_3$).

Compound ***8c***. White powder; melting point: 261−262 °C; isolated yield: 814 mg (84%); HRMS [ESI-MS, positive

https://doi.org/10.1021/acsomega.3c05020
ACS Omega 2023, 8, 35283−35294

mode]: MF: $C_{28}H_{32}N_2O_5S$; observed m/z 509.2081 $[M + H]^+$ [calcd. 509.2110]; ^1H NMR (400 MHz, pyridine-d_5): δ 11.85 (1H, s, −NH), 8.60 (d, J = 7.5 Hz, 1H), 8.60 (s, 1H), 7.57 (s, 1H), 7.49 (d, J = 5.9 Hz, 1H), 6.84 (s, 1H), 6.01 (d, J = 5.9 Hz, 1H), 4.67 (d, J = 6.0 Hz, 1H), 4.65−4.57 (m, 1H), 4.15 (d, J = 6.1 Hz, 1H), 3.82−3.76 (m, 1H), 3.77−3.71 (m, 1H), 3.63−3.57 (m, 2H), 3.12 (dd, J = 9.0, 5.9 Hz, 1H), 3.02 (dd, J = 13.0, 8.7 Hz, 1H), 2.47−2.35 (m, 3H), 2.20 (s, 3H), 1.95−1.83 (m, 1H), 1.64 (dd, J = 13.0, 4.7 Hz, 2H), 1.30 (s, 3H), 1.05 (t, J = 3.6 Hz, 1H), 0.97 (d, J = 7.6 Hz, 3H); ^{13}C NMR (100 MHz, pyridine-d_5): δ 211.89 (−C═O), 179.58(−C═O), 178.95 (−C═O), 165.04(−CH), 140.63 (−C), 133.10 (−CH), 132.10 (−C), 131.53 (−CH), 125.47 (−CH), 124.70(−CH), 119.63 (−C), 84.43 (−C), 79.47 (−CH), 75.72 (−C), 66.58 (−CH), 65.25 (−C), 59.80 (−C), 49.67 (−CH), 49.67 ($-CH_2$), 40.92 (−CH), 35.66($-CH_2$), 32.70 ($-CH_2$), 32.57 ($-CH_2$), 23.43 ($-CH_2$), 21.52 ($-CH_3$), 20.65 ($-CH_3$), 18.36($-CH_3$), 17.23($-CH_3$).

Compound ***8d***. White powder; melting point: 217−218 °C; isolated yield: 716 mg (73%); HRMS [ESI-MS, positive mode]: MF: $C_{26}H_{27}ClN_2O_5S$; observed m/z 515.1410 $[M + H]^+$ [calcd. 515.1407]; ^1H NMR (400 MHz, pyridine-d_5): δ 12.29 (1H, s, −NH), 7.59−7.55 (m, 1H), 7.35−7.28 (m, 2H), 6.70−6.67 (m, 1H), 6.15−6.06 (m, 1H), 4.79 (d, J = 5.7 Hz, 1H), 4.82−4.75 (m, 1H), 4.49−4.43 (m, 1H), 3.98 (dd, J = 11.1, 5.2 Hz, 1H), 3.89−3. 81 (m, 2H), 3.50−3.42 (m, 1H), 3.16−3.09 (m, 1H), 2.87 (dd, J = 13.0, 8.0 Hz, 1H), 2.56−2.38 (m, 3H), 1.99−1.90 (m, 1H), 1.82−1.66 (m, 2H), 1.29 (s, 3H), 1.00 (d, J = 7.1 Hz, 3H); ^{13}C NMR (100 MHz, pyridine-d_5): δ 212.22 (−C═O), 178.92(−C═O), 178.69 (−C═O), 165.70(−CH), 143.38 (−C), 131.65 (−CH), 131.35 (−CH), 128.51 (−CH), 128.19 (−C), 127.62(−C), 112.30 (−CH), 84.81 (−C), 79.91 (−CH), 75.18 (−C), 67.39 (−CH), 66.17 (−C), 60.21 (−C), 50.41 ($-CH_2$), 49.35 (−CH), 41.25 (−CH), 36.38 ($-CH_2$), 33.29 ($-CH_2$), 33.05 ($-CH_2$), 23.53 ($-CH_2$), 20.95 ($-CH_3$), 18.79($-CH_3$).

Compound ***8e***. White powder; melting point: 218−219 °C; isolated yield: 883 mg (83%); HRMS [ESI-MS, positive mode]: MF: $C_{26}H_{27}BrN_2O_5S$; observed m/z 559.0904 $[M + H]^+$ [calcd. 559.0902]; ^1H NMR (400 MHz, pyridine-d_5): δ 12.28 (1H, s, −NH), 7.59 (d, J = 5.9 Hz, 1H), 7.31−7.19 (m, 1H), 6.67 (d, J = 8.3 Hz, 1H), 6.13 (d, J = 5.9 Hz, 1H), 4.80 (d, J = 5.8 Hz, 1H), 4.50−4.44 (m, 1H), 3.98 (dd, J = 11.4, 5.5 Hz, 1H), 3.85 (dd, J = 17.4, 7.1 Hz, 2H), 3.46 (dd, J = 15.9, 7.2 Hz, 1H), 3.13 (dd, J = 9.2, 6.2 Hz, 1H), 2.87 (dd, J = 13.1, 7.9 Hz, 1H), 7.50−2.38(m, 3H), 2.00−1.91 (m, 1H), 1.82−1.79 (m, 1H), 1.69 (dd, J = 12.4, 5.0 Hz, 1H), 1.29 (s, 3H), 1.02 (d, J = 7.2 Hz, 3H); ^{13}C NMR (100 MHz, pyridine-d_5): δ 211.25 (−C═O), 177.80 (−C═O), 177.68 (−C═O), 164.77 (−CH), 142.81 (−C), 133.26 (−CH), 130.65 (−CH), 130.26 (−CH), 126.97(−C), 114.65 (−C), 111.83-(−CH), 84.81 (−C), 78.94 (−CH), 75.19 (−C), 66.42 (−CH), 65.14 (−C), 59.21 (−C), 49.54 ($-CH_2$), 48.26 (−CH), 40.24 (−CH), 35.43($-CH_2$), 32.37 ($-CH_2$), 32.07 ($-CH_2$), 22.54 ($-CH_2$), 19.95 ($-CH_3$), 17.83($-CH_3$).

Compound ***9***. Yellow crystals; melting point: 237−238 °C; isolated yield: 762 mg (81%); HRMS [ESI-MS, positive mode]: MF: $C_{27}H_{27}NO_6S$; observed m/z 494.1636 $[M + H]^+$ [calcd. 494.1637]; ^1H NMR (400 MHz, pyridine-d_5): δ 7.95−7.90 (m, 1H), 7.67 (d, J = 5.9 Hz, 1H), 7.62−7.58 (m, 2H), 7.57−7.51 (m, 1H), 7.46 (s, 1H), 6.27 (d, J = 5.9 Hz, 1H), 4.99 (d, J = 6.9 Hz, 1H), 4.30−4.24 (m, 2H), 4.17 (d, J = 7.7 Hz, 1H), 3.88 (d, J = 7.7 Hz, 1H), 3.56 (t, J = 9.7 Hz, 1H), 3.10 (dd, J = 9.9, 5.4 Hz, 1H), 2.97 (dd, J = 13.5, 8.6 Hz, 1H), 2.66−2.54 (m, 1H), 2.49 (dd, J = 13.3, 5.9 Hz, 2H), 2.09−1.94 (m, 1H), 1.74 (d, J = 12.0 Hz, 2H), 1.23 (s, 3H), 1.04 (d, J = 7.6 Hz, 3H); ^{13}C NMR (100 MHz, pyridine-d_5): δ 213.68 (−C═O), 200.91 (−C═O), 199.01 (−C═O), 176.41(−C═O), 167.37 (−CH), 141.99 (−C), 138.96 (−CH), 138.49 (−CH), 131.90 (−CH), 124.62 (−CH), 124.29 (−CH), 85.12 (−C), 82.60 (−C), 81.17 (−CH), 69.93 (−CH), 68.46 (−C), 60.69 (−C), 52.19 ($-CH_2$), 46.34 (−CH), 41.27 (−CH), 38.66($-CH_2$), 35.03 ($-CH_2$), 32.88 ($-CH_2$), 23.89 ($-CH_2$), 20.29 ($-CH_3$), 18.81($-CH_3$).

Compound ***10a***. White powder; melting point: 289−290 °C; isolated yield: 635 mg (70%) HRMS [ESI-MS, positive mode]: MF: $C_{28}H_{32}N_2O_5$; observed m/z 477.2389 $[M + H]^+$ [calcd. 477.2389]; ^1H NMR (400 MHz, pyridine-d_5): δ 11.87 (1H, s, −NH), 7.79 (d, J = 7.0 Hz, 1H), 7.51 (d, J = 5.9 Hz, 1H), 7.19 (td, J = 7.7, 1.3 Hz, 2H), 7.03 (td, J = 7.6, 1.0 Hz, 1H), 6.64 (d, J = 7.7 Hz, 1H), 6.05 (d, J = 5.9 Hz, 1H), 4.58 (d, J = 5.9 Hz, 1H), 3.88−3.81 (m, 1H), 3.69−3.64 (m, 1H), 2.90 (dd, J = 12.7, 9.4 Hz, 1H), 2.50−2.31 (m, 4H), 2.25 (dd, J = 12.6, 6.2 Hz, 1H), 2.02−1.86 (m, 4H), 1.73 (d, J = 12.9 Hz, 1H), 1.64 (dd, J = 13.0, 4.4 Hz, 1H), 1.53−1.45 (m, 1H), 1.34 (s, 3H), 1.33−1.27 (m, 2H), 0.98 (d, J = 7.7 Hz, 3H); ^{13}C NMR (100 MHz, pyridine-d_5): δ 211.90 (−C═O), 179.51 (−C═O), 178.60 (−C═O), 165.10 (−CH), 144.69 (−C), 131.27 (−CH), 130.46 (−CH), 126.96 (−CH), 126.62 (−CH), 123.20 (−CH), 110.20 (−CH), 84.55 (−C), 78.91 (−CH), 78.52 (−C), 60.99 (−C), 59.78 (−C), 59.78 (−CH), 49.39 (−CH), 46.72 ($-CH_2$), 40.91 (−CH), 34.53 ($-CH_2$), 32.74 ($-CH_2$), 32.30 ($-CH_2$), 26.29 ($-CH_2$), 25.79 ($-CH_2$), 23.83 ($-CH_2$), 20.86 ($-CH_3$),18.42($-CH_3$).

Compound ***10b***. White powder; melting point: 294−295 °C; isolated yield: 753 mg (78%) HRMS [ESI-MS, positive mode]: MF: $C_{29}H_{34}N_2O_6$; observed m/z 507.2498 $[M + H]^+$ [calcd. 507.2495]; ^1H NMR (400 MHz, pyridine-d_5): δ 11. (1H, s, −NH), 7.79 (d, J = 7.0 Hz, 1H), 7.56 (d, J = 5.9 Hz, 1H), 7.50 (d, J = 2.6 Hz, 1H), 6.90 (dd, J = 8.4, 2.6 Hz, 1H), 6.65 (d, J = 8.4 Hz, 1H), 6.07 (d, J = 5.9 Hz, 1H), 7.28 (s, 1H), 4.59 (d, J = 5.8 Hz, 1H), 3.89−3.81 (m, 1H), 3.69 (s, 3H), 3.66−3.62 (m, 1H), 2.90 (dd, J = 12.6, 9.4 Hz, 1H), 2.56−2.54 (m, 1H), 2.48−2.34 (m, 4H), 2.25 (dd, J = 12.6, 6.2 Hz, 2H), 1.96−1.85 (m, 4H), 1.33 (s, 3H), 1.29−1.28 (m, 2H), 1.00 (d, J = 7.5 Hz, 3H); ^{13}C NMR (100 MHz, pyridine-d_5): δ 212.06 (−C═O), 179.74 (−C═O), 178.69 (−C═O), 165.37 (−CH), 156.96 (−C), 138.04 (−C), 131.36 (−CH), 128.27 (−C), 116.32 (−CH), 113.41 (−CH), 110.83 (−CH), 84.85 (−C), 79.13 (−CH), 79.01 (−C), 61.29 (−C), 59.99 (−CH), 59.86 (−C), 56.53 ($-CH_3$), 49.47 (−CH), 46.93-($-CH_2$), 40.98 (−CH), 34.63 ($-CH_2$), 32.85 ($-CH_2$), 32.40($-CH_2$), 26.42 ($-CH_2$), 25.89 ($-CH_2$), 23.89 ($-CH_2$), 20.92 ($-CH_3$),18.59 ($-CH_3$).

Compound ***10c***. White powder; melting point: 256−257 °C; isolated yield: 877 mg (83%); HRMS [ESI-MS, positive mode]: MF: $C_{28}H_{31}BrN_2O_5$; observed m/z 555.1489 $[M + H]^+$ [calcd. 555.1495]; ^1H NMR (400 MHz, pyridine-d_5): δ 12.15 (1H, s, −NH), 8.01 (d, J = 1.8 Hz, 1H), 7.49 (d, J = 5.9 Hz, 1H), 7.46−7.43 (m, 1H), 7.45 (dd, J = 8.2, 2.0 Hz, 1H), 6.56 (d, J = 8.2 Hz, 1H), 6.05 (d, J = 5.9 Hz, 1H), 4.59 (d, J = 5.7 Hz, 1H), 3.84−3.77 (m, 1H), 3.65 (dd, J = 11.5, 5.7 Hz, 1H), 2.84 (dd, J = 12.6, 9.3 Hz, 1H), 2.46−2.30 (m, 5H), 2.25 (dd, J = 12.7, 6.4 Hz, 1H), 1.95−1.81 (m, 4H), 1.72 (d, J = 12.9 Hz, 1H), 1.63 (dd, J = 12.9, 4.8 Hz, 1H), 1.36−1.32 (m, 2H), 1.29 (s, 3H), 0.97 (s, 3H); ^{13}C NMR (100 MHz, pyridine-d_5): δ

https://doi.org/10.1021/acsomega.3c05020
ACS Omega 2023, 8, 35283−35294

211.71 (−C═O), 179.15 (−C═O), 178.19 (−C═O), 165.05 (−CH), 143.94 (−C), 133.35 (−CH), 131.26 (−CH), 129.59 (−C), 129.47 (−CH), 115.75 (−CH), 111.84 (−CH), 84.50 (−C), 78.98 (−CH), 78.43 (−C), 61.44 (−C), 59.90 (−CH), 49.41 (−CH), 46.76 ($-CH_2$), 40.85 (−CH), 34.38 ($-CH_2$), 32.72 ($-CH_2$), 32.25 ($-CH_2$), 26.18 ($-CH_2$), 25.62 ($-CH_2$), 23.68 ($-CH_2$), 20.72 ($-CH_3$),18.39 ($-CH_3$).

Compound ***10d***. White powder; melting point: 255−256 °C; isolated yield: 700 mg (72%) HRMS [ESI-MS, positive mode]: MF: $C_{28}H_{31}ClN_2O_5$; observed *m*/*z* 511.2006 [M + H]$^+$ [calcd. 511.2000]; ^{1}H NMR (400 MHz, pyridine-d_5): δ 12.14 (1H, s, −NH), 7.87 (d, *J* = 2.0 Hz, 1H), 7.52−7.48 (m, 1H), 7.32−7.28 (m, 1H), 6.62−6.59 (m, 1H), 6.07−6.05 (m, 1H), 4.59 (d, *J* = 5.7 Hz, 1H), 3.84−3.77 (m, 1H), 3.66 (dd, *J* = 10.8, 5.0 Hz, 1H), 2.85 (dd, *J* = 12.6, 9.4 Hz, 1H), 2.45−2.31 (m, 5H), 2.25 (dd, *J* = 12.7, 6.4 Hz, 1H), 1.98−1.97 (m, 1H), 1.92−1.82 (m, 4H), 1.72 (d, *J* = 13.0 Hz, 1H), 1.63 (dd, *J* = 12.7, 4.2 Hz, 1H), 1.37−1.33 (m, 1H), 1.30 (s, 3H), 0.97 (d, *J* = 7.6 Hz, 3H); ^{13}C NMR (100 MHz, pyridine-d_5): δ 211.78 (−C═O), 179.16 (−C═O), 178.35 (−C═O), 165.11 (−CH), 143.51 (−C), 131.27 (−CH), 130.47 (−CH), 129.26 (−C), 128.29 (−C), 126.72 (−CH), 111.39 (−CH), 84.51 (−C), 78.99 (−CH), 78.47 (−C), 61.45 (−C), 59.90 (−CH), 59.75 (−C), 49.43 (−CH), 46.78 ($-CH_2$), 40.86 (−CH), 34.39 ($-CH_2$), 32.73 ($-CH_2$), 32.27 ($-CH_2$), 26.21 ($-CH_2$), 25.63 ($-CH_2$), 23.68 ($-CH_2$), 20.76 ($-CH_3$), 18.41 ($-CH_3$).

Compound ***10e***. White powder; melting point: 217−218 °C; isolated yield: 748 mg (80%) HRMS [ESI-MS, positive mode]: MF: $C_{29}H_{34}N_2O_5$; observed *m*/*z* 491.2545 [M + H]$^+$ [calcd. 491.2546]; ^{1}H NMR (400 MHz, pyridine-d_5): δ 11.77 (1H, s, −NH), 7.66 (s, 1H), 7.50 (d, *J* = 5.9 Hz, 1H), 7.19 (s, 1H), 7.03 (dd, *J* = 7.8, 0.9 Hz, 1H), 6.60 (d, *J* = 7.8 Hz, 1H), 6.04 (d, *J* = 5.9 Hz, 1H), 4.59 (d, *J* = 5.9 Hz, 1H), 3.89−3.84 (m, 1H), 3.69−3.62 (m, 1H), 2.91 (dd, *J* = 12.6, 9.4 Hz, 1H), 2.56 (d, *J* = 7.8 Hz, 1H), 2.46−2.35 (m, 3H), 2.27 (dd, *J* = 12.6, 6.2 Hz, 1H), 2.17 (s, 3H), 1.98−1.89 (m, 4H), 1.74 (d, *J* = 12.8 Hz, 1H), 1.64 (dd, *J* = 13.4, 4.4 Hz, 1H), 1.58−1.50 (m, 1H), 1.39−1.35 (m, 2H), 1.32 (s, 3H), 0.97 (d, *J* = 7.7 Hz, 3H); ^{13}C NMR (100 MHz, pyridine-d_5): δ 211.64 (−C═O), 179.33 (−C═O), 178.30 (−C═O), 164.80 (−CH), 141.98 (−C), 132.08 (−C), 131.01 (−CH), 130.54 (−CH), 126.93 (−CH), 126.75 (−C), 109.69 (−CH), 84.27 (−C), 78.64 (−CH), 78.39 (−C), 60.76 (−C), 59.60 (−CH), 59.52 (−C), 49.15 (−CH), 46.53($-CH_2$), 40.65 (−CH), 34.28 ($-CH_2$), 32.48 ($-CH_2$), 32.08 ($-CH_2$), 26.06 ($-CH_2$), 25.55 ($-CH_2$), 23.52 ($-CH_2$), 21.35 ($-CH_3$), 20.58 ($-CH_3$),18.16 ($-CH_3$).

Compound ***13a***. White powder; melting point: 242−243 °C; isolated yield: 665 mg (80%); HRMS [ESI-MS, positive mode]: MF: $C_{25}H_{28}N_2O_5$; observed *m*/*z* 437.2072 [M + H]$^+$ [calcd. 437.2076]; ^{1}H NMR (400 MHz, Pyridine-d_5): δ 11.92 (1H, s, −NH), 7.77 (d, *J* = 7.4 Hz, 1H), 7.49 (d, *J* = 5.9 Hz, 1H), 7.17 (s, 1H), 7.13−7.10 (m, 1H), 7.00 (t, *J* = 7.3 Hz, 1H), 6.61 (d, *J* = 7.6 Hz, 1H), 6.06 (d, *J* = 5.8 Hz, 1H), 4.45 (d, *J* = 6.2 Hz, 1H), 3.90 (dd, *J* = 14.1, 8.0 Hz, 1H), 3.53 (dd, *J* = 11.1, 6.2 Hz, 1H), 3.47−3.42 (m, 1H), 3.16 (td, *J* = 11.6, 6.0 Hz, 1H), 2.41−2.33 (m, 3H), 2.26 (s, 3H), 2.04−1.95 (m, 1H), 1.80 (dd, *J* = 14.2, 5.0 Hz, 1H), 1.59 (dd, *J* = 12.4, 5.3 Hz, 1H), 1.35 (s, 3H), 0.97 (d, *J* = 7.5 Hz, 3H); ^{13}C NMR (100 MHz, pyridine-d_5): δ 211.89 (−C═O), 179.13 (−C═O), 178.76 (−C═O), 164.99 (−CH), 144.52 (−C), 131.33 (−CH), 130.58 (−CH), 127.01 (−C), 126.43 (−CH), 123.20 (−CH), 110.28 (−CH), 84.43 (−C), 79.13 (−CH), 78.29 (−C), 61.86 (−C), 59.77 (−C), 52.12 ($-CH_2$), 48.68 (−CH), 40.94 (−CH), 36.20 ($-CH_3$), 32.63 ($-CH_2$), 28.28 ($-CH_2$), 23.52 ($-CH_2$), 20.65 ($-CH_3$),18.29 ($-CH_3$).

Compound ***13b***. White powder; melting point: 226−227 °C; isolated yield: 804 mg (82%); HRMS [ESI-MS, positive mode]: MF: $C_{25}H_{27}BrN_2O_5$; observed *m*/*z* 515.1182 [M + H]$^+$ [calcd. 515.1182]; ^{1}H NMR (400 MHz, pyridine-d_5): δ 12.13 (1H, s, −NH), 7.94 (d, *J* = 1.9 Hz, 1H), 7.55 (d, *J* = 5.9 Hz, 1H), 7.37 (dd, *J* = 8.2, 2.0 Hz, 1H), 7.19 (s, 1H), 6.58 (d, *J* = 8.2 Hz, 1H), 6.10 (d, *J* = 5.9 Hz, 1H), 4.46 (d, *J* = 6.1 Hz, 1H), 3.94−3.81 (m, 1H), 3.50 (dd, *J* = 11.9, 6.1 Hz, 1H), 3.44−3.39 (m, 1H), 3.11 (td, *J* = 11.7, 5.9 Hz, 1H), 2.45−2.32 (m, 3H), 2.25 (s, 3H), 2.05−1.94 (m, 1H), 1.80−1.75 (m, 1H), 1.62 (dd, *J* = 12.7, 4.7 Hz, 1H), 1.32 (s, 3H), 1.00 (d, *J* = 7.5 Hz, 3H); ^{13}C NMR (100 MHz, pyridine-d_5): δ 211.45 (−C═O), 178.48 (−C═O), 178.18 (−C═O), 164.77 (−CH), 143.53 (−C), 133.26 (−CH), 131.10 (−CH), 129.34 (−C), 129.05 (−CH), 115.51 (−C), 111.73 (−CH), 84.19 (−C), 78.99 (−CH), 78.04 (−C), 62.01 (−C), 59.49 (−C), 51.95 ($-CH_2$), 48.43 (−CH), 40.65 (−CH), 35.96 ($-CH_3$), 32.40 ($-CH_2$), 27.98 ($-CH_2$), 23.22 ($-CH_2$), 20.30 ($-CH_3$),18.06 ($-CH_3$).

Compound ***13c***. White powder; melting point: 291−292 °C; isolated yield: 669 mg (78%) HRMS [ESI-MS, positive mode]: MF: $C_{26}H_{30}N_2O_5$; observed *m*/*z* 451.2232 [M + H]$^+$ [calcd. 451.2233]; ^{1}H NMR (400 MHz, Pyridine-d_5): δ 11.79 (1H, s, −NH), 7.63 (s, 1H), 7.49 (d, *J* = 7.4 Hz, 1H), 7.15 (s, 1H), 6.95 (m, 1H), 6.57 (t, *J* = 7.4 Hz, 1H), 6.05 (d, *J* = 5.5 Hz, 1H), 4.44 (s, 1H), 3.94 (s, 1H), 3.54−3.51 (m, 1H), 3.50−3.47 (m, 1H), 3.22−3.16 (m, 1H), 2.38−2.36 (m, 3H), 2.32 (d, *J* = 3.5 Hz, 3H), 2.19 (d, *J* = 4.1 Hz, 3H), 1.98 (d, *J* = 5.0 Hz, 1H), 1.80 (d, *J* = 14.4 Hz, 1H), 1.61−1.58 (m, 1H), 1.33 (d, *J* = 3.9 Hz, 3H), 0.97 (s, 3H); ^{13}C NMR (100 MHz, pyridine-d_5): δ 211.65 (−C═O), 178.81 (−C═O), 178.61 (−C═O), 164.73 (−CH), 141.79 (−C), 132.20 (−C), 131.09 (−CH), 130.67 (−CH), 126.75 (−CH × 2), 109.77 (−CH), 84.16 (−C), 78.86 (−CH), 78.13 (−C), 61.62 (−C), 59.51 (−C), 51.94 ($-CH_2$), 48.39 (−CH), 40.70 (−CH), 36.04 ($-CH_3$), 32.39 ($-CH_2$), 28.03 ($-CH_2$), 23.23 ($-CH_2$), 21.26 ($-CH_3$), 20.38 ($-CH_3$), 18.11 ($-CH_3$).

Compound ***13d***. White powder; melting point: 262−263 °C; isolated yield: 672 mg (75%) HRMS [ESI-MS, positive mode]: MF: $C_{25}H_{27}ClN_2O_5$; observed *m*/*z* 471.1696 [M + H]$^+$ [calcd. 471.1687]; ^{1}H NMR (400 MHz, pyridine-d_5): δ 12.14 (1H, s, −NH), 7.82 (d, *J* = 1.8 Hz, 1H), 7.51 (d, *J* = 5.9 Hz, 1H), 7.21 (dd, *J* = 8.2, 2.0 Hz, 1H), 7.18 (s, 1H), 6.58 (d, *J* = 8.2 Hz, 1H), 6.08 (d, *J* = 5.9 Hz, 1H), 4.46 (d, *J* = 6.1 Hz, 1H), 4.09 (q, *J* = 7.1 Hz, 1H), 3.91−3.83 (m, 1H), 3.51 (dd, *J* = 11.6, 6.0 Hz, 1H), 3.42 (dd, *J* = 13.6, 5.4 Hz, 1H), 3.44−3.39 (m, 1H), 3.11 (td, *J* = 11.7, 5.9 Hz, 1H), 2.39−2.32 (m, 4H), 2.25 (s, 3H), 2.03−1.93 (m, 1H), 1.80−1.75 (m, 1H), 1.61 (dd, *J* = 12.4, 5.1 Hz, 1H), 1.32 (s, 3H), 0.98 (d, *J* = 7.4 Hz, 3H); ^{13}C NMR (100 MHz, pyridine-d_5): δ 211.52 (−C═O), 178.62 (−C═O), 178.19 (−C═O), 164.83 (−CH), 143.08 (−C), 131.11 (−CH), 130.37 (−CH), 129.00 (−C), 128.10 (−C), 126.27 (−CH), 111.27 (−CH), 84.20 (−C), 78.99 (−CH), 78.07 (−C), 62.03 (−C), 59.51 (−C), 51.95 ($-CH_2$), 48.47 (−CH), 40.67 (−CH), 35.97 ($-CH_3$), 32.41 ($-CH_2$), 27.98 ($-CH_2$), 23.21 ($-CH_2$), 20.33 ($-CH_3$), 18.08 ($-CH_3$).

Compound ***13e***. White powder; melting point: 282−283 °C; isolated yield: 693 mg (78%); HRMS [ESI-MS, positive mode]: MF: $C_{26}H_{30}N_2O_6$; observed *m*/*z* 467.2189 [M + H]$^+$ [calcd. 467.2182]; ^{1}H NMR (400 MHz, pyridine-d_5): δ 11.75

https://doi.org/10.1021/acsomega.3c05020
ACS Omega 2023, 8, 35283−35294

(1H, s, −NH), 7.52−7.50 (m, 1H), 7.17 (s, 1H), 6.84 (dd, J = 8.4, 2.6 Hz, 1H), 6.59 (d, J = 8.4 Hz, 1H), 6.07 (d, J = 5.9 Hz, 1H), 4.44 (d, J = 6.1 Hz, 1H), 3.94−3.89 (m, 1H), 3.72 (s, 3H), 3.55−3.45 (m, 2H), 3.18 (td, J = 11.6, 6.0 Hz, 1H), 2.41−2.36 (m, 3H), 2.33 (s, 3H), 2.05−1.95 (m, 1H), 1.80 (dd, J = 14.3, 5.0 Hz, 2H), 1.60 (dd, J = 11.9, 5.0 Hz, 1H), 1.33 (s, 3H), 0.98 (d, J = 7.4 Hz, 4H); ^{13}C NMR (100 MHz, pyridine-d_5): δ 211.68 (−C═O), 178.81 (−C═O), 178.65 (−C═O), 164.84 (−CH), 156.74 (−C), 137.54 (−C), 131.12 (−CH), 127.88 (−C), 116.67 (−CH), 112.59 (−CH), 110.65 (−CH), 84.20 (−C), 78.98 (−CH), 78.48 (−C), 61.83 (−C), 59.53 (−C), 56.32 ($-CH_3$), 51.99 ($-CH_2$), 48.40 (−CH), 40.72 (−CH), 36.09 ($-CH_3$), 32.43 ($-CH_2$), 28.06 ($-CH_2$), 23.25 ($-CH_2$), 20.38 ($-CH_3$),18.11 ($-CH_3$).

Compound ***14***. Yellow crystals; melting point: 249−250 °C; isolated yield: 625 mg (73%) HRMS [ESI-MS, positive mode]: MF: $C_{26}H_{27}NO_6$; observed m/z 450.1913 $[M + H]^+$ [calcd. 450.1917]; ^{1}H NMR (400 MHz, pyridine-d_5): δ 7.93−7.90 (m, 1H), 7.77 (dd, J = 7.5, 0.9 Hz, 1H), 7.56 (d, J = 5.9 Hz, 1H), 7.52 (dd, J = 7.5, 1.2 Hz, 1H), 7.49 (dd, J = 7.4, 1.2 Hz, 1H), 6.17 (d, J = 5.9 Hz, 1H), 4.88 (d, J = 6.6 Hz, 1H), 3.71−3.62 (m, 2H), 3.32 (td, J = 8.7, 5.8 Hz, 1H), 2.86−2.80 (m, 1H), 2.64−2.58 (m, 1H), 2.42−2.33 (m, 2H), 2.32 (s, 3H), 2.02−1.93 (m, 1H), 1.68−1.58 (m, 2H), 1.29 (s, 3H), 0.99 (d, J = 7.8 Hz, 3H); ^{13}C NMR (100 MHz, pyridine-d_5): δ 211.61 (−C═O), 201.19 (−C═O), 199.98 (−C═O), 176.31 (−C═O), 165.05 (−CH), 144.92 (−C), 141.31 (−C), 137.35 (−CH), 136.81 (−CH), 131.13 (−CH), 123.28 (−CH), 122.74 (−CH), 83.95 (−C), 80.35 (−C), 79.47 (−CH), 62.27 (−C), 59.79 (−C), 52.62 ($-CH_2$), 46.02 (−CH), 40.70 (−CH), 36.13 ($-CH_3$), 32.09 ($-CH_2$), 29.73 ($-CH_2$), 22.96 ($-CH_2$), 19.65 ($-CH_3$),17.87 ($-CH_3$).

Cell Lines and Culture Conditions. Human cancer cell lines, namely, HCT-116 (colon), MCF-7 (breast), Mia-Paca (pancreas), and A549 (lungs), were obtained from the National Centre for Cell Science (NCCS), Pune. The cell lines were grown in RPMI-1640 medium containing 1% penicillin and streptomycin and 10% fetal bovine serum albumin (FBS). The cell lines were maintained in a controlled atmosphere of 95% air and 5% CO_2 gas and at a temperature of 37 °C using a CO_2 incubator (New Brunswick, Galaxy 170R, Eppendorf, Stevenage, U.K.). Storage of the media was performed at 2−8 °C.

Cytotoxicity Profile against Human Cancer Cell Lines by the SRB Assay. The SRB assay was performed wherein 100 μL of cell suspension was given to each well of the 96-well tissue culture plate. After 24 h incubation of the cell suspension, the test sample was added in a complete growth medium (100 μL). The plates were incubated for 48 h in a carbon dioxide incubator. After that, to stop cell growth, trichloroacetic acid (50%, 50 μL) was added to each and every well. By incubating these plates at 4 °C for 1 h, the fixation of the cells to the bottom of the well was accomplished. To remove trichloroacetic acid, the plates were cleaned three times with tap water and air-dried. Then, for staining the plates, sulforhodamine-B dye (0.4% in 1% acetic acid, 100 μL) was used for 30 min. Again, the plates were washed three times with 1% acetic acid and then air-dried. The adsorbed dye was solubilized with Tris−HCl Buffer (100 mL, 0.01M, pH 10.4), and a mechanical stirrer was used to stir the plates gently for 10 min. An enzyme-linked immunosorbent assay (ELISA) reader (Thermo Scientific) was used to record absorbance at 540 nm. The IC_{50} was determined using Graph perturbed angular distribution (PAD) Prism Software Version 5.0.

■ ASSOCIATED CONTENT

Supporting Information

The Supporting Information is available free of charge at https://pubs.acs.org/doi/10.1021/acsomega.3c05020.

Crystallographic data of compound **4a** (CIF)
Crystallographic data of compounds **6** (CIF)
Crystallographic data of compound **8d** (CIF)
Crystallographic data of compound **8e** (CIF)
Crystallographic data of compounds **9** (CIF)
Crystallographic data of compounds **14** (CIF)
^{1}H and ^{13}C NMR, 2D NMR, IR, and HRMS spectral information on all compounds of this article can be found in the online version (PDF)

■ AUTHOR INFORMATION

Corresponding Authors

Abhijit Hazra − *National Institute of Pharmaceutical Education and Research (NIPER), Kolkata 700054, India;* orcid.org/0000-0003-1094-549X; Email: apuhazra@gmail.com

Yogesh P. Bharitkar − *CSIR-Indian Indian Institute of Integrative Medicine, Jammu 180001, India; Academy of Scientific and Innovative Research (AcSIR), Ghaziabad 201002, India;* orcid.org/0000-0001-6371-0972; Email: yogeshp.bharitkar@iiim.res.in, yogeshbharitkar@gmail.com

Authors

Chetan Paul Singh − *CSIR-Indian Indian Institute of Integrative Medicine, Jammu 180001, India; Academy of Scientific and Innovative Research (AcSIR), Ghaziabad 201002, India*

Priyanka Sharma − *National Institute of Pharmaceutical Education and Research (NIPER), Kolkata 700054, India*

Manzoor Ahmed − *CSIR-Indian Indian Institute of Integrative Medicine, Jammu 180001, India; Academy of Scientific and Innovative Research (AcSIR), Ghaziabad 201002, India*

Diljeet Kumar − *CSIR-Indian Indian Institute of Integrative Medicine, Jammu 180001, India; Academy of Scientific and Innovative Research (AcSIR), Ghaziabad 201002, India*

Yogesh Brijwashi Sharma − *National Institute of Pharmaceutical Education and Research (NIPER), Kolkata 700054, India*

Jayanta Samanta − *Department of Chemistry, SRM Institute of Science and Technology, Kattankulathur 603 203 Tamil Nadu, India;* orcid.org/0000-0003-4104-4774

Zabeer Ahmed − *CSIR-Indian Indian Institute of Integrative Medicine, Jammu 180001, India; Academy of Scientific and Innovative Research (AcSIR), Ghaziabad 201002, India*

Sanket Kumar Shukla − *CSIR-Indian Indian Institute of Integrative Medicine, Jammu 180001, India; Academy of Scientific and Innovative Research (AcSIR), Ghaziabad 201002, India*

Complete contact information is available at: https://pubs.acs.org/10.1021/acsomega.3c05020

Notes

The authors declare no competing financial interest.

https://doi.org/10.1021/acsomega.3c05020
ACS Omega 2023, 8, 35283−35294

■ ACKNOWLEDGMENTS

CPS thanks CSIR, Govt. of India, for providing fellowship. M.A. and D.K. thank UGC, Govt. of India, for providing a fellowship. The authors also acknowledge the director of CSIR-IIIM Jammu and Director, NIPER-Kolkata for providing laboratory facilities. The authors also acknowledge the Nanotechnology Research Centre (NRC), SRMIST for providing the research facilities. The authors greatly acknowledge Dr. Ramalingam Natarajan, Senior Principal Scientist, CSIR-IICB, for supporting with X-ray diffraction data. IIIM Publication Number: CSIR-IIIM/IPR/00593

■ REFERENCES

(1) Atanasov, A. G.; Zotchev, S. B.; Dirsch, V. M. International Natural Product Sciences Taskforce; Supuran, C. T. Natural products in drug discovery: advances and opportunities. *Nat. Rev. Drug Discovery* **2021**, *20* (3), 200−216.

(2) Bednarek, P.; Osbourn, A. Plant-Microbe Interactions: Chemical Diversity in Plant Defense. *Science* **2009**, *324* (5928), 746−748.

(3) Thompson, L. A.; Ellman, J. A. Synthesis and Applications of Small Molecule Libraries. *Chem. Rev.* **1996**, *96* (1), 555−600.

(4) Nielsen, J. Combinatorial Synthesis of Natural Products. *Curr. Opin. Chem. Biol.* **2002**, *6* (3), 297−305.

(5) Liu, R.; Li, X.; Lam, K. S. Combinatorial Chemistry in Drug Discovery. *Curr. Opin. Chem. Biol.* **2017**, *38*, 117−126.

(6) Tietze, L. F.; Bell, H. P.; Chandrasekhar, S. Natural Product Hybrids as New Leads for Drug Discovery. *Angew. Chem., Int. Ed.* **2003**, *42* (34), 3996−4028.

(7) Henrich, C. J.; Beutler, J. A. Matching the Power of High Throughput Screening to the Chemical Diversity of Natural Products. *Nat. Prod. Rep.* **2013**, *30* (10), 1284−1298.

(8) Majhi, S.; Das, D. Chemical Derivatization of Natural Products: Semisynthesis and Pharmacological Aspects- A Decade Update. *Tetrahedron* **2021**, *78*, No. 131801.

(9) Newman, D. J.; Cragg, G. M. Natural Products as Sources of New Drugs over the Nearly Four Decades from 01/1981 to 09/2019. *J. Nat. Prod.* **2020**, *83* (3), 770−803.

(10) Galloway, W. R. J. D.; Isidro-Llobet, A.; Spring, D. R. Diversity-Oriented Synthesis as a Tool for the Discovery of Novel Biologically Active Small Molecules. *Nat. Commun.* **2010**, *1* (1), No. 80.

(11) Mortensen, K. T.; Osberger, T. J.; King, T. A.; Sore, H. F.; Spring, D. R. Strategies for the Diversity-Oriented Synthesis of Macrocycles. *Chem. Rev.* **2019**, *119* (17), 10288−10317.

(12) Saha, S.; Acharya, C.; Pal, U.; Chowdhury, S. R.; Sarkar, K.; Maiti, N. C.; Jaisankar, P.; Majumder, H. K. Novel Spirooxindole Derivative Inhibits the Growth of Leishmania Donovani Parasites Both In Vitro and In Vivo by Targeting Type IB Topoisomerase. *Antimicrob. Agents Chemother.* **2016**, *60*, 6281−6293.

(13) Panda, S. S.; Girgis, A. S.; Aziz, M. N.; Bekheit, M. S. Spirooxindole: A Versatile Biologically Active Heterocyclic Scaffold. *Molecules* **2023**, *28*, 618.

(14) Marti, C.; Carreira, E. M. Total Synthesis of (−)-Spirotryprostatin B: Synthesis and Related Studies. *J. Am. Chem. Soc.* **2005**, *127*, 11505−11515.

(15) Borthwick, A. D. 2,5-Diketopiperazines: Synthesis, Reactions, Medicinal Chemistry, and Bioactive Natural Products. *Chem. Rev.* **2012**, *112*, 3641−3716.

(16) Hong, S.; Jung, M.; Park, Y.; Ha, M. W.; Park, C.; Lee, M.; Park, H. G. *Efficient* Enantioselective Total Synthesis of (−)-Horsfiline. *Chem.− Eur. J.* **2013**, *19*, 9599−9605.

(17) Yu, B.; Yu, D.-Q.; Liu, H.-M. Spirooxindoles: Promising Scaffolds for Anticancer Agents. *Eur. J. Med. Chem.* **2015**, *97*, 673−698.

(18) Pavlovska, T. L.; Redkin, R. G.; Lipson, V. V.; Atamanuk, D. V. Molecular Diversity of Spirooxindoles. Synthesis and Biological Activity. *Mol. Diversity* **2016**, *20* (1), 299−344.

(19) Galliford, C. V.; Scheidt, K. A. Pyrrolidinyl-Spirooxindole Natural Products as Inspirations for the Development of Potential Therapeutic Agents. *Angew. Chem., Int. Ed.* **2007**, *46* (46), 8748−8758.

(20) Zhao, Y.; Liu, L.; Sun, W.; Lu, J.; McEachern, D.; Li, X.; Yu, S.; Bernard, D.; Ochsenbein, P.; Ferey, V.; Carry, J.-C.; Deschamps, J. R.; Sun, D.; Wang, S. Diastereomeric Spirooxindoles as Highly Potent and Efficacious MDM2 Inhibitors. *J. Am. Chem. Soc.* **2013**, *135* (19), 7223−7234.

(21) Ding, K.; Lu, Y.; Nikolovska-Coleska, Z.; Qiu, S.; Ding, Y.; Gao, W.; Stuckey, J.; Krajewski, K.; Roller, P. P.; Tomita, Y.; Parrish, D. A.; Deschamps, J. R.; Wang, S. Structure-Based Design of Potent Non-Peptide MDM2 Inhibitors. *J. Am. Chem. Soc.* **2005**, *127* (29), 10130−10131.

(22) Lotfy, G.; Aziz, Y. M. A.; Said, M. M.; El Ashry, E. S. H.; El Tamany, E. S. H.; Abu-Serie, M. M.; Teleb, M.; Dömling, A.; Barakat, A. Molecular Hybridization Design and Synthesis of Novel Spirooxindole-Based MDM2 Inhibitors Endowed with BCL2 Signaling Attenuation; a Step towards the next Generation P53 Activators. *Bioorg. Chem.* **2021**, *117*, No. 105427.

(23) Islam, M. S.; Al-Majid, A. M.; Sholkamy, E. N.; Barakat, A.; Viale, M.; Menichini, P.; Speciale, A.; Loiacono, F.; Azam, M.; Verma, V. P.; Yousuf, S.; Teleb, M. Optimized Spirooxindole-Pyrazole Hybrids Targeting the P53-MDM2 Interplay Induce Apoptosis and Synergize with Doxorubicin in A549 Cells. *Sci. Rep.* **2023**, *13* (1), No. 7441.

(24) Zhang, Q.; Zeng, S. X.; Lu, H. Targeting P53-MDM2-MDMX Loop for Cancer Therapy. *Subcell. Biochem.* **2014**, *85*, 281−319.

(25) Zhao, Y.; Yu, S.; Sun, W.; Liu, L.; Lu, J.; McEachern, D.; Shargary, S.; Bernard, D.; Li, X.; Zhao, T.; Zou, P.; Sun, D.; Wang, S. A Potent Small-Molecule Inhibitor of the MDM2−P53 Interaction (MI-888) Achieved Complete and Durable Tumor Regression in Mice. *J. Med. Chem.* **2013**, *56* (13), 5553−5561.

(26) Hazra, A.; Paira, P.; Sahu, K. B.; Naskar, S.; Saha, P.; Paira, R.; Mondal, S.; Maity, A.; Luger, P.; Weber, M.; Mondal, N. B.; Banerjee, S. Chemistry of Andrographolide: Formation of Novel Di-Spiropyrrolidino and Di-Spiropyrrolizidino-Oxindole Adducts via One-Pot Three-Component [3 + 2] Azomethine Ylide Cycloaddition. *Tetrahedron Lett.* **2010**, *51* (12), 1585−1588.

(27) Hazra, A.; Bharitkar, Y. P.; Chakraborty, D.; Mondal, S. K.; Singal, N.; Mondal, S.; Maity, A.; Paira, R.; Banerjee, S.; Mondal, N. B. Regio- and Stereoselective Synthesis of a Library of Bioactive Dispiro-Oxindolo/Acenaphthoquino Andrographolides via 1,3-Dipolar Cycloaddition Reaction Under Microwave Irradiation. *ACS Comb. Sci.* **2013**, *15* (1), 41−48.

(28) Bharitkar, Y. P.; Kanhar, S.; Suneel, N.; Mondal, S. K.; Hazra, A.; Mondal, N. B. Chemistry of Withaferin-A: Chemo, Regio, and Stereoselective Synthesis of Novel Spiro-Pyrrolizidino-Oxindole Adducts of Withaferin-A via One-Pot Three-Component [3 + 2] Azomethine Ylide Cycloaddition and Their Cytotoxicity Evaluation. *Mol. Diversity* **2015**, *19* (2), 251−261.

(29) Dey, S. K.; Bose, D.; Hazra, A.; Naskar, S.; Nandy, A.; Munda, R. N.; Das, S.; Chatterjee, N.; Mondal, N. B.; Banerjee, S.; Saha, K. D. Cytotoxic Activity and Apoptosis-Inducing Potential of Di-Spiropyrrolidino and Di-Spiropyrrolizidino Oxindole Andrographolide Derivatives. *PLoS One* **2013**, *8* (3), No. e58055.

(30) Chakraborty, D.; Maity, A.; Jain, C. K.; Hazra, A.; Bharitkar, Y. P.; Jha, T.; Majumder, H. K.; Roychoudhury, S.; Mondal, N. B. Cytotoxic Potential of Dispirooxindolo/Acenaphthoquino Andrographolide Derivatives against MCF-7 Cell Line. *MedChemComm* **2015**, *6* (4), 702−707.

(31) Singh, M.; Ravichandiran, V.; Bharitkar, Y. P.; Hazra, A. Natural Products Containing Olefinic Bond: Important Substrates for Semi-Synthetic Modification Towards Value Addition. *Curr. Org. Chem.* **2020**, *24* (7), 709−745.

(32) Singh, M.; Hirlekar, B. U.; Mondal, S.; Pant, S.; Dhaked, D. K.; Ravichandiran, V.; Hazra, A.; Bharitkar, Y. P. Isolation of Phytochemicals from Dolichandrone Atrovirens Followed by Semi-synthetic Modification of Ixoside via Azomethine Ylide Cyclo-

https://doi.org/10.1021/acsomega.3c05020
ACS Omega 2023, 8, 35283−35294

addition; Computational Approach towards Chemo-Selection. *Nat. Prod. Res.* **2023**, *37* (13), 2215−2224.
(33) Kaur, L.; Malhi, D. S.; Cooper, R.; Kaur, M.; Sohal, H. S.; Mutreja, V.; Sharma, A. Comprehensive Review on Ethnobotanical Uses, Phytochemistry, Biological Potential and Toxicology of *Parthenium Hysterophorus* L.: A Journey from Noxious Weed to a Therapeutic Medicinal Plant. *J. Ethnopharmacol.* **2021**, *281*, No. 114525.
(34) Oudhia, P. Medicinal uses of Congress weed *Parthenium Hysterophorus* L.: A review. *Ecol., Environ. Conserv.* **2001**, *7*, 175−177.
(35) Patel, S. Harmful and Beneficial Aspects of *Parthenium Hysterophorus*: An Update. *3 Biotech* **2011**, *1* (1), 1−9.
(36) Kaur, A.; Kaur, S.; Jandrotia, R.; Singh, H. P.; Batish, D. R.; Kohli, R. K.; Rana, V. S.; Shakil, N. A. Parthenin—A Sesquiterpene Lactone with Multifaceted Biological Activities: Insights and Prospects. *Molecules* **2021**, *26* (17), No. 5347.
(37) Balaich, J. N.; Mathias, D. K.; Torto, B.; Jackson, B. T.; Tao, D.; Ebrahimi, B.; Tarimo, B. B.; Cheseto, X.; Foster, W. A.; Dinglasan, R. R. The Nonartemisinin Sesquiterpene Lactones Parthenin and Parthenolide Block Plasmodium Falciparum Sexual Stage Transmission. *Antimicrob. Agents Chemother.* **2016**, *60* (4), 2108−2117.
(38) Moujir, L.; Callies, O.; Sousa, P. M. C.; Sharopov, F.; Seca, A. M. L. Applications of Sesquiterpene Lactones: A Review of Some Potential Success Cases. *Appl. Sci.* **2020**, *10* (9), No. 3001.

https://doi.org/10.1021/acsomega.3c05020
ACS Omega 2023, 8, 35283−35294